11. Minor Planet Electronic Circ. 1997-C12 (1997).
12. Hogg, D. W., Quinlan, G. D. & Tremaine, S. Dynamical limits on dark mass in the outer solar system. *Astron. J.* **101,** 2274–2286 (1991).
13. Whipple, F. L. A comet model I: the acceleration of comet Encke. *Astrophys. J.* **111,** 375–394 (1950).
14. Kuiper, G. P. in *Astrophysics* (ed. Hynek, J. A.) 357–424 (McGraw-Hill, New York, 1951).
15. Ip, W.-H. Dynamical processes of macro-accretion of Uranus and Neptune—a first look. *Icarus* **80,** 167–178 (1989).
16. Ip, W.-H. & Fernández, J. A. Steady-state injection of short-period comets from the trans-Neptunian cometary belt. *Icarus* **92,** 185–193 (1991).
17. Torbett, M. Chaotic motion in a comet disk beyond Neptune—the delivery of short-period comets. *Astron. J.* **98,** 1477–1482 (1989).
18. Morbidelli, A. & Valsecchi, G. Neptune scattered planetesimals could have sculpted the primordial Kuiper belt. *Icarus* (submitted).
19. Duncan, M. & Levison, H. *Science* (submitted).
20. Morbidelli, A., Thomas, F. & Moons, M. The resonant structure of the Kuiper belt and the dynamics of the first five trans-Neptunian objects. *Icarus* **118,** 322–340 (1996).

Acknowledgements. We thank M. Holman for discussions, G. Williams for providing Fig. 2, and W. Brown for help with the observations.

Correspondence and requests for materials should be addressed to J.L. (e-mail: luu@cfa.harvard.edu).

Experimental evidence for non-exponential decay in quantum tunnelling

Steven R. Wilkinson, Cyrus F. Bharucha, Martin C. Fischer, Kirk W. Madison, Patrick R. Morrow, Qian Niu, Bala Sundaram* & Mark G. Raizen

Department of Physics, The University of Texas at Austin, Austin, Texas 78712-1081, USA

An exponential decay law is the universal hallmark of unstable systems and is observed in all fields of science. This law is not, however, fully consistent with quantum mechanics and deviations from exponential decay have been predicted for short as well as long times[1–8]. Such deviations have not hitherto been observed experimentally. Here we present experimental evidence for short-time deviation from exponential decay in a quantum tunnelling experiment. Our system consists of ultra-cold sodium atoms that are trapped in an accelerating periodic optical potential created by a standing wave of light. Atoms can escape the wells by quantum tunnelling, and the number that remain can be measured as a function of interaction time for a fixed value of the well depth and acceleration. We observe that for short times the survival probability is initially constant before developing the characteristics of exponential decay. The conceptual simplicity of the experiment enables a detailed comparison with theoretical predictions.

We consider the motion of ultra-cold atoms in an accelerating optical potential of the form $V_0\cos[2k_Lx - k_Lat^2]$, where a is the acceleration, V_0 is the well depth, x is position in the laboratory frame, t is time and k_L is the laser wavenumber[9,10]. In the accelerating reference frame (x'), this potential becomes $V_0\cos(2k_Lx') + Max'$ where M is the mass of the atom. The linear term in x' leads to an asymmetry in the potential wells. This 'washboard potential' is the same as for the condensed-matter system of an electron moving in a periodic lattice with a d.c. electric field. The periodic optical potential is created by the spatially varying field of a standing wave of light formed by two counter-propagating beams from a single-mode laser. The laser is tuned sufficiently far from atomic resonance so that spontaneous scattering can be neglected, and the atom remains in the ground state. The standing wave is accelerated by ramping the frequency difference of its two beams.

In our previous work on quantum transport of atoms in an accelerating potential, we performed a spectroscopic study of the band structure and observed Wannier–Stark ladder resonances[11]. In parallel to our work, Bloch oscillations of ultra-cold atoms were also directly observed[12]. Those experiments were done in a regime where tunnelling from the trapped state was negligible. Recently we studied the tunnelling process for larger accelerations, and showed that it is the ultimate limit for this atom accelerator[13]. The trapped state can be considered an unstable quantum system that decays into a reservoir. This can be seen in the 'washboard potential' of the co-moving frame: an atom, trapped in one of the wells, escapes via tunnelling to the continuum. The predicted deviation from exponential decay for short times is related to the fact that the coupling between the system and reservoir is still reversible during that stage. Moreover, the decayed and undecayed state are not yet resolvable, even in principle. In the present system, it is not possible to tell whether an atom is still tracking the accelerating lattice for short times; only in longer times can this question by answered. By then, the decay is irreversible, leading to an exponential decay law. A significant improvement in the signal-to-noise ratio of the data has now enabled us to resolve the short-time tunnelling probability and to observe this phenomenon.

To trap and accelerate a significant number of atoms in a weak potential requires the initial source of atoms to be ultra-cold. We achieve this using a magneto-optic trap consisting of six intersecting

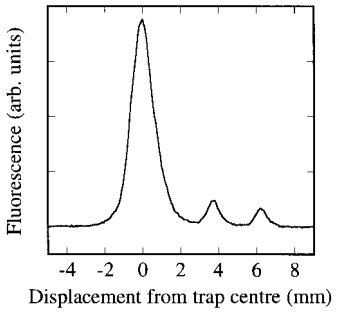

Figure 1 Distribution of atoms after exposure to a three-stage accelerating standing wave for $V_0/h = 80$ kHz. A small acceleration of 1,500 m s^{-2} was first imposed to trap atoms and separate them from the rest of the distribution. A large acceleration of 7,000 m s^{-2} was then turned on for a duration of 34 μs. During this stage atoms tunnel from the trapped state, and are lost to the accelerating potential. Finally the same small acceleration was imposed to separate the atoms that have survived from those that have tunnelled out. The duration of the three-step process is 1.5 ms, and the total switching time between the three stages is under 500 ns. A free drift of 3 ms allowed the surviving atoms to separate spatially from the main distribution.

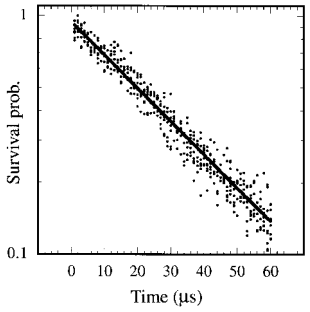

Figure 2 Typical example of experimentally measured survival probability for a small acceleration of 1,200 m s^{-2}, a large acceleration of 4,500 m s^{-2}, and $V_0/h = 50$ kHz as a function of the duration of the large acceleration. Note that the vertical axis is logarithmic. The solid line is a fit to an exponential.

* Present address: Department of Mathematics, CSI-CUNY, Staten Island, New York 10314, USA.

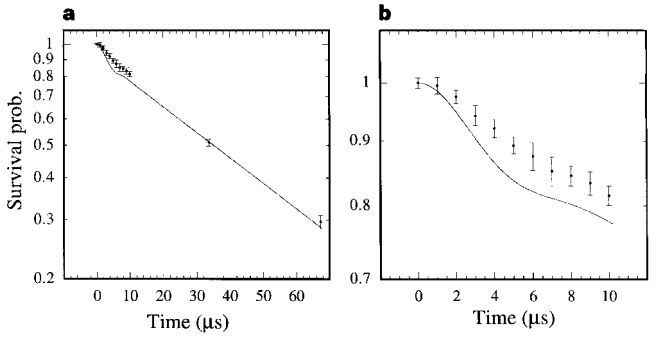

Figure 3 Survival probability as a function of duration of the large acceleration. The experimental data are shown with error bars (one standard deviation). The solid line is the theoretical prediction. For these data the acceleration was 7,000 m s^{-2}, and the potential was $V_0/h = 85 \pm 8.5$ kHz. The theoretical calculation used the same acceleration, but the potential was taken as $V_0/h = 74$ kHz.

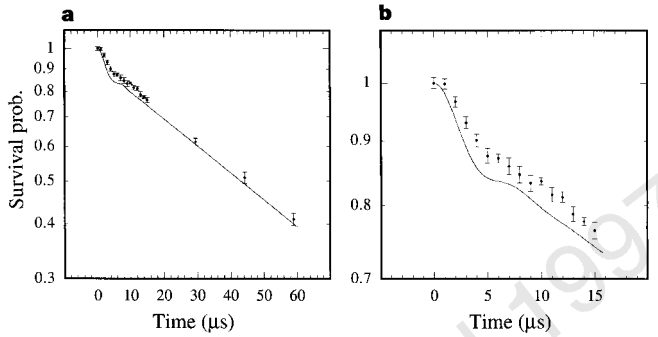

Figure 4 Survival probability as a function of duration of the large acceleration. The experimental data are shown with error bars. The solid line is the theoretical prediction. For these data the acceleration was 9,000 m s^{-2}, and the potential was $V_0/h = 90 \pm 9$ kHz. The theoretical calculation used the same acceleration, but the potential was taken as $V_0/h = 92$ kHz.

laser beams superimposed on a magnetic field gradient to trap and cool sodium atoms[14]. With this configuration, we trap $\sim 10^5$ atoms within a gaussian distribution of position ($\sigma = 0.17$ mm) and momentum ($\sigma = 4.6\,\hbar k_L$). The details of our experimental set-up for trapping and cooling have been described elsewhere[15].

The accelerating standing wave is provided by a separate stabilized single-mode dye laser tuned far (up to 20 GHz) from atomic resonance. The output beam from this laser is split into two beams. Each beam is aligned through an acousto-optic modulator that controls its frequency. Both beams are spatially filtered and aligned on the trapped atoms in a counter-propagating configuration, with a beam waist of 1.9 mm in the centre of the trap. When the two beams are at the same frequency, the resulting standing wave is stationary in the laboratory frame. A linear ramp of 4 MHz in 200 μs creates an accelerating potential of 6,000 m s^{-2}.

To study tunnelling in this system, atoms are first trapped and cooled in the magneto-optic trap during a loading time of 6 s. The trapping beams as well as the magnetic field gradient are then turned off, and the accelerating one-dimensional potential is turned on. A three-step acceleration is implemented to measure the loss due to tunnelling[13]. A small acceleration is first imposed to trap atoms and separate them from the rest of the distribution. A large acceleration is then turned on for a controlled duration τ. During this stage, atoms tunnel from the trapped state and are lost to the accelerating potential. Finally the same small acceleration is imposed to separate the atoms that have survived from those that have tunnelled out. Once the final velocity is reached, the potential is turned off, allowing a 3-ms free drift. The six beams of the magneto-optic trap are then turned on in zero magnetic field. Atomic motion is effectively frozen at this stage, and the resonance fluorescence is recorded on a charged-coupled-device (CCD) camera. The resulting two-dimensional images are binned in the direction orthogonal to the standing wave to obtain one-dimensional distributions, as shown in Fig. 1. The large peak on the left is from atoms in the initial distribution that were not trapped, the middle peak is from atoms that tunnelled during the second step of large acceleration, and the peak on the right is from atoms that survived the large acceleration. The integrated area of the peak on the right is normalized to the total area contained in the middle and right peaks, in order to determine the fraction of survivors.

We have measured the survival probability as a function of τ and find an exponential decay law, as shown for a particular case in Fig. 2. The uncertainty is due primarily to laser power fluctuations, but we were able to obtain very good fits to an exponential decay law. We have conducted a detailed study of the decay rates as a function of acceleration and well depth, and find good agreement with a quantum simulation[13]. This process can also be modelled as a Landau–Zener tunnelling process which gives an analytic expression for the tunnelling rate that is in reasonable agreement with experiment.

To observe short-time deviations from the exponential decay, the power of each beam in the standing wave was measured on a photodiode and digitized. In the data analysis we then selected runs for which the power fluctuations were within a ±1% window. The exponential fit was not appreciably altered as the fluctuations were reduced, but the short-time deviation was resolved. Our results are shown in Fig. 3 for an acceleration of 7,000 m s^{-2} and in Fig. 4 for an acceleration of 9,000 m s^{-2}. Each point represents (on the average) 20 experimental runs, and the error bar is one standard deviation about the mean. Data were taken at intervals of 1 μs for the first 15 μs to obtain the highest resolution in short time. The long-time exponential behaviour was extensively tested in earlier work[13], and the data shown here for times longer than 15 μs establish the exponents. Figures 3b and 4b show expanded-scale views of the short-time behaviour. The focus of our attention is on timescales shorter than 15 μs. The initial survival probability is flat, owing to a reversible coupling to the bath. The intermediate stage is characterized by a sharper fall-off than the exponential. This can be understood as a 'projection loss' due to a mismatch between trapped states at the two values of the acceleration. Beyond this stage, an irreversible coupling to the reservoir leads to exponential decay.

The theoretical analysis of this problem and comparison with our data proceeds along two directions. The first is a numerical simulation of the time-dependent Schrödinger equation to determine the decay constant for the exponential stage. We find good quantitative agreement with our measurements with no adjustable parameters[13]. To analyse the short-time tunnelling probability and the approach to exponential decay, we use a simple model that provides analytical expressions, and find good agreement with experiment. The starting point for this analysis is the energy structure of a periodic lattice, which consists of energy bands separated by bandgaps. This structure can be represented as a dispersion relation between the energy and quasi-momentum, k. As a familiar point of reference, free-particle motion would be represented as a parabola in this picture as the energy is proportional to the square of the momentum. When an acceleration is imposed, k varies in time as the atom moves through the band. To obtain a simple expression for the tunnelling probability during the stage of large acceleration, we keep only the first bandgap, and

neglect the second and higher gaps. This leads to a modified band structure with a single band, separated by a bandgap from free particle motion. This approximation is valid when the tunnelling rate across the higher gaps is sufficiently high, as is the case in the present work. We treat the non-adiabatic coupling between the trapped and non-trapped states as a weak perturbation, and find that the logarithm of the survival probability in the trapped state is to leading order

$$\ln P(t) = -\int_0^t \mathrm{d}\tau (t-\tau) W(\tau) \tag{1}$$

where

$$W(\tau) = \frac{a^2}{2V_0}\int_{-\infty}^{\infty}\mathrm{d}s \frac{1}{1+(s-a\tau/V_0)^2}\frac{1}{1+s^2} \times \cos\left(\frac{V_0^2}{a}\int_{s-a\tau/V_0}^{s}\sqrt{1+z^2}\,\mathrm{d}z\right) \tag{2}$$

In the above expressions, time t is measured in units of $M/4\hbar k_L^2$, the potential amplitude V_0 in $4\hbar^2 k_L^2/M$, and acceleration in $8\hbar^2 k_L^3/M^2$. As $W(\tau)$ decays to zero sufficiently fast for large τ, the long-time behaviour of the survival probability is exponential, $P(t) = \exp(-\alpha t + \beta)$, where α and β are the infinite time integrals of $W(\tau)$ and $\tau W(\tau)$, respectively. In this system there is no long-time deviation from exponential decay, because with a tilted potential the energy spectrum is not bounded from below. On the other hand, $W(\tau)$ is finite for $\tau = 0$, showing that equation (1) is quadratic at short times. Equation (1) is plotted in Figs 3 and 4, and demonstrates good overall agreement with the experimental results. The theory predicts a somewhat larger projection loss than the observed values. This due to the fact that the theory assumes zero acceleration in the first and third stages, creating a larger mismatch between the trapped state in the second stage. We also find that the analytic approximations become better at larger values of the acceleration where Landau–Zener theory is a good model for the tunnelling process.

Here we have reported observed short-time deviation from exponential decay in a tunnelling experiment. In the future we will investigate the possibility of suppressing tunnelling by repeated measurements during the non-exponential time[6,7]. □

Received 27 January; accepted 28 April 1997.

1. Khalfin, L. A. Contribution to the decay theory of a quasi-stationary state. *JETP* **6,** 1053–1063 (1958).
2. Winter, R. G. Evolution of a quasi-stationary state. *Phys. Rev.* **123,** 1503–1507 (1961).
3. Fonda, L., Ghirardi, G. C. & Rimini, A. Decay theory of unstable quantum systems. *Rep. Prog. Phys.* **41,** 587–631 (1978).
4. Ballentine, L. E. *Quantum Mechanics* (Prentice Hall, Englewood Cliffs, NJ, 1990).
5. Greenland, P. T. Seeking non-exponential decay. *Nature* **335,** 298 (1988).
6. Chiu, C. B., Sudarshan, E. C. G. & Misra, B. Time evolution of unstable quantum states and a resolution of Zeno's paradox. *Phys. Rev. D* **16,** 520–529 (1977).
7. Sudarshan, E. C. G., Chiu, C. B. & Bhamathi, G. in *Advances in Chemical Physics* Vol. XCIX (eds Prigogine, I. & Rice, S. A.) 121–209 (Wiley, New York, 1997).
8. Petrosky, T. & Prigogine, I. in *Advances in Chemical Physics* Vol. XCIX (eds Prigogine, I. & Rice, S. A.) 1–120 (Wiley, New York, 1997).
9. Kazantsev, A. P., Surdutovich, G. I. & Yakovlev, V. P. *Mechanical Action of Light on Atoms* (World Scientific, Singapore, 1990).
10. Niu, Q., Zhao, X., Georgakis, G. A. & Raizen, M. G. Atomic Landau-Zener tunneling and Wannier-Stark ladders in optical potential. *Phys. Rev. Lett.* **76,** 4504–4507 (1996).
11. Wilkinson, S. R., Bharucha, C. F., Madison, K. W., Niu, Q. & Raizen, M. G. Observation of atomic Wannier-Stark ladders in an accelerating optical potential. *Phys. Rev. Lett.* **76,** 4512–4515 (1996).
12. Ben Dahan, M., Peik, E., Reichel, J., Castin, Y. & Salomon, C. Bloch oscillations of atoms in an optical potential. *Phys. Rev. Lett.* **76,** 4508–4511 (1996).
13. Bharucha, C. F. *et al.* Observation of atomic tunneling in an accelerating optical potential. *Phys. Rev. A* **55,** R857–R860 (1997).
14. Cohen-Tannoudji, C. in *Fundamental Systems in Quantum Optics* (eds Dalibard, J., Raimond, J. M. & Zinn-Justin, J.) 1–164 (Elsevier, Amsterdam, 1992).
15. Moore, F. L., Robinson, J. C., Bharucha, C., Williams, P. E. & Raizen, M. G. Observation of dynamical localization in atomic momentum transfer: a new testing ground for quantum chaos. *Phys. Rev. Lett.* **73,** 2974–2977 (1994).

Acknowledgements. M.G.R. was supported by the US Office of Naval Research, the Robert A. Welch Foundation, and the US National Science Foundation; B.S. was supported by the US National Science Foundation; Q.N. was supported by the Robert A. Welch Foundation.

Correspondence should be addressed to M.G.R. (e-mail: raizen@physics.utexas.edu).

Chiral discrimination using piezoelectric and optical gas sensors

K. Bodenhöfer, A. Hierlemann*, J. Seemann, G. Gauglitz, B. Koppenhoefer† & W. Göpel

Institute of Physical and Theoretical Chemistry, Centre of Interface Analysis and Sensors, and † Institute of Organic Chemistry, University of Tübingen, Auf der Morgenstelle 8, D-72076 Tübingen, Germany

Odour perception in humans can sometimes discriminate different enantiomers of a chiral compound[1–3], such as limonene. Chiral discrimination represents one of the greatest challenges in attempts to devise selective and sensitive gas sensors. The importance of such discrimination for pharmacology is clear, as the physiological effect of enantiomers of drugs and other biologically active molecules may differ significantly[4]. Here we describe two different sensor systems that are capable of recognizing different enantiomers and of qualitatively monitoring the enantiomeric composition of amino-acid derivatives and lactates in the gas phase. One sensor detects changes in mass, owing to binding of the compound being analysed (the 'analyte'), by thickness shear-mode resonance[5–7]; the other detects changes in the thickness of a surface layer by reflectometric interference spectroscopy[8–10]. Both devices use the two enantiomers of a chiral polymeric receptor, and offer rapid on-line detection of chiral species with high selectivity.

Natural odour receptors are proteins that use only one enantiomeric form (the L form) of the amino-acid building blocks[11,12]. In contrast, our sensors apply both enantiomers of a receptor simultaneously. We use the chiral model receptor octyl-Chirasil-Val (Fig. 1), which is derived from the well-known chiral chromatographic stationary phase Chirasil-Val[13]. It contains chiral peptide residues for enantiomer recognition and non-chiral lipophilic side chains[14]. Solutions of these polymers were sprayed onto the quartz plates (by airbrush)[7] or spin-cast on the optical devices[10]. The layer thickness ranged between 100 and 300 nm. In addition to the two sets of chiral sensors, reference devices coated with the non-enantioselective polymer poly(dimethylsiloxane) (SE-30) were included in the sensor arrays to recognize artefacts caused by fluctuating gas-phase concentrations or contaminations of the (*S*)- and (*R*)-analytes.

Signal transduction (chemical to electrical) was achieved using thickness shear-mode resonators (TSMRs; fundamental frequency, 30 MHz) and reflectometric interference spectroscopy (RIFS) techniques (Fig. 2). When the polymer-coated TSMRs are exposed to analyte gas, sorption of molecules by the polymer generates a change of the oscillating mass which causes a shift of the operating frequency[5–7]. The sorption strength depends on the interaction mechanisms (H-bridge bonds, dispersion forces) between matrix and analyte molecules. Reflectometric interference spectroscopy was applied to characterize changes in the optical thickness $\Delta(nd)$, where n is refractive index, and d is layer thickness of the polymer layer (swelling on analyte sorption). Interferograms produced by the reflection of light at the multi-layer system glass/polymer/air (Fig. 2) were evaluated[8–10].

All the sensors were mounted in the same flow-through cell and simultaneously exposed to analyte gas at a constant temperature of 303 K. The chiral analytes included both enantiomers of *N*-trifluoroacetyl-alanin methyl ester (*N*-TFA-Ala-OMe, ref. 15, Figs 1 and 3), ethyl lactate and methyl lactate (Fig. 4). The test vapours were generated by thermally controlled vaporizers using synthetic air as carrier gas. Typical experiments consisted of